

Somatostatin Presynaptically Inhibits Both GABA and Glutamate Release Onto Rat Basal Forebrain Cholinergic Neurons

Toshihiko Momiyama and Laszlo Zaborszky

J Neurophysiol 96:686-694, 2006. First published Mar 29, 2006; doi:10.1152/jn.00507.2005

You might find this additional information useful...

This article cites 43 articles, 16 of which you can access free at:

<http://jn.physiology.org/cgi/content/full/96/2/686#BIBL>

Updated information and services including high-resolution figures, can be found at:

<http://jn.physiology.org/cgi/content/full/96/2/686>

Additional material and information about *Journal of Neurophysiology* can be found at:

<http://www.the-aps.org/publications/jn>

This information is current as of February 13, 2007 .

Somatostatin Presynaptically Inhibits Both GABA and Glutamate Release Onto Rat Basal Forebrain Cholinergic Neurons

Toshihiko Momiyama^{1,2} and Laszlo Zaborszky³

¹Division of Cerebral Structure, National Institute for Physiological Sciences, Okazaki; ²Core Research for Evolutional Science and Technology, Japan Science and Technology Corporation, Kawaguchi, Japan; and ³Center for Molecular and Behavioral Neuroscience, Rutgers, The State University of New Jersey, Newark, New Jersey

Submitted 16 May 2005; accepted in final form 24 March 2006

Momiyama, Toshihiko and Laszlo Zaborszky. Somatostatin presynaptically inhibits both GABA and glutamate release onto rat basal forebrain cholinergic neurons. *J Neurophysiol* 96: 686–694, 2006; doi:10.1152/jn.00507.2005. A whole cell patch-clamp study was carried out in slices obtained from young rat brain to elucidate the roles of somatostatin in the modulation of synaptic transmission onto cholinergic neurons in the basal forebrain (BF), a region that contains cholinergic and GABAergic corticopetal neurons and somatostatin (SS)-containing local circuit neurons. Cholinergic neurons within the BF were identified by *in vivo* prelabeling with Cy3 IgG. Because in many cases SS is contained in GABAergic neurons in the CNS, we investigated whether exogenously applied SS can influence GABAergic transmission onto cholinergic neurons. Bath application of somatostatin (1 μ M) reduced the amplitude of the evoked GABAergic inhibitory presynaptic currents (IPSCs) in cholinergic neurons. SS also reduced the frequency of miniature IPSCs (mIPSCs) without affecting their amplitude distribution. SS-induced effect on the mIPSC frequency was significantly larger in the solution containing 7.2 mM Ca^{2+} than in the standard (2.4 mM Ca^{2+}) external solution. Similar effects were observed in the case of non-NMDA glutamatergic excitatory postsynaptic currents (EPSCs). SS inhibited the amplitude of evoked EPSCs and reduced the frequency of miniature EPSCs dependent on the external Ca^{2+} concentration with no effect on their amplitude distribution. Pharmacological analyses using SS-receptor subtype-specific drugs suggest that SS-induced action of the IPSCs is mediated mostly by the *sst*₂ subtype, whereas *sst* subtypes mediating SS-induced inhibition of EPSCs are mainly *sst*₁ or *sst*₄. These findings suggest that SS presynaptically inhibits both GABA and glutamate release onto BF cholinergic neurons in a Ca^{2+} -dependent way, and that SS-induced effect on IPSCs and EPSCs are mediated by different *sst* subtypes.

INTRODUCTION

The basal forebrain (BF) is a region in the forebrain that contains cholinergic and GABAergic corticopetal neurons in addition to various local circuit neurons (Zaborszky and Duque 2000, 2003). Loss of BF cholinergic neurons and concomitant deficits in cholinergic markers in the cortex constitute a hallmark of Alzheimer's disease (AD) (Price et al. 1986). Studies combining EEG, juxtacellular labeling of recorded neurons with subsequent identification of their transmitter in anesthetized rats (Duque et al. 2000; Manns et al. 2000), or selective lesioning of the cholinergic neurons in combination with EEG monitoring during the sleep–wake cycle (Kapas et al. 1996) indicate that the generation of neocortical activation critically depends on cholinergic inputs from these regions.

Address for reprint requests and other correspondence: T. Momiyama, Division of Cerebral Structure, National Institute for Physiological Sciences, Myodaiji, Okazaki 444-8787, Japan (E-mail: tmomi@nips.ac.jp).

Alterations in somatostatin (SS) levels and SS neuronal morphology have been observed in the cortex and BF of AD patients (Candy et al. 1983; Davies and Terry 1981; Francis et al. 1987; Kowall and Beal 1988; Roberts et al. 1985; Rossor et al. 1980). Behavioral experiments in rats suggests that mnemonic functions are impaired by depleting SS from central stores and this effect is mediated in part through the BF cholinergic system (Haroutunian et al. 1989). Intracerebroventricular application or microinjection of SS-receptor agonists in forebrain areas result in sleep suppression (Obal and Krueger 2003).

Neurons expressing SS constitute a peptidergic interneuronal system in the septum, striatum, hippocampus, and cerebral cortex (Chesselet and Graybiel 1986; Forloni et al. 1990; Kohler and Eriksson; 1984; Vincent et al. 1985). In BF areas, patches of SS fibers and axons of local SS neurons were observed in close vicinity to cholinergic neurons (Zaborszky and Duque 2000), indicating a potential effect of SS on cholinergic neurons. Cholinergic neurons receive GABAergic input in BF areas (Zaborszky et al. 1986) and SS perikarya have been shown to be coexpressed with γ -aminobutyric acid (GABA) in many forebrain areas (Esclapez and Houser 1995; Hendry et al. 1984; Kosaka et al. 1988; Somogyi et al. 1984). A direct glutamate effect on cholinergic neurons is suggested by the presence of Vglut1- and Vglut2-type synapses on BF cholinergic neurons (Zaborszky et al. 2003). Although these morphological data raise the possibility of interactions among acetylcholine (ACh), SS, glutamate, and GABA, little information has been available regarding the functional role of SS in BF regions. Therefore using whole cell patch-clamp technique in forebrain slices of young rats, we investigated the effect of exogenously applied SS on GABAergic and glutamatergic transmission onto BF cholinergic neurons. Cholinergic neurons were identified by *in vivo* prelabeling with Cy3-192IgG, a selective marker of p75 neurotrophin receptor-expressing neurons (Wu et al. 2000). Preliminary data were previously published in abstract form (Momiyama and Zaborszky 2002, 2004).

METHODS

Labeling of BF cholinergic neurons with Cy3-192IgG for electrophysiology

All experiments were carried out in accordance with the Guiding Principles for the Care and Use of Animals in the Field of Physio-

The costs of publication of this article were defrayed in part by the payment of page charges. The article must therefore be hereby marked "advertisement" in accordance with 18 U.S.C. Section 1734 solely to indicate this fact.

logical Sciences of the Physiological Society of Japan (1998) and the UK Animals (Scientific Procedures) Act 1986. Young rats (10- to 14-days-old) were anesthetized with pentobarbital (50 mg/kg, administered intraperitoneally) and then mounted into a stereotaxic apparatus. Cy3-192IgG (3–4 μ l; 0.4 mg/ml) was injected unilaterally into the lateral ventricle of each rat using a Hamilton syringe (22-gauge needle) at a rate of 0.5 μ l/min (Wu et al. 2000). The coordinates of the lateral ventricle used were 0.9 mm posterior from bregma, 1.1–1.2 mm lateral from midline, and 4 mm below from the dura.

Slice preparation for patch-clamp recordings

Three to six days after intracerebroventricular injection of Cy3-192IgG, rats were killed by decapitation under deep halothane anesthesia and coronal slices, containing the basal forebrain regions including the substantia innominata (SI) and the horizontal limb of the diagonal band (HDB), were cut (300 μ m thick) using a microslicer (DTK-1000 or PRO7, Dosaka, Kyoto, Japan) in ice-cold oxygenated cutting Krebs solution of the following composition (in mM): NaCl, 124; KCl, 3; CaCl₂, 0.5; MgCl₂, 6; NaH₂PO₄, 1; NaHCO₃, 26; and D-glucose, 10; pH adjusted by 95% O₂-5% CO₂. The slices were then transferred to a holding chamber containing standard Krebs solution of the following composition (in mM): NaCl, 124; KCl, 3; CaCl₂, 2.4; MgCl₂, 1.2; NaH₂PO₄, 1; NaHCO₃, 26; and D-glucose, 10; pH 7.4 when bubbled with 95% O₂-5% CO₂. Slices were incubated in the holding chamber at room temperature (21–26°C) for \geq 1 h before recording.

Whole cell recording and data analysis

For recording, slices were transferred to the recording chamber, held submerged, and superfused with standard Krebs solution (bubbled with 95% O₂-5% CO₂) at a rate of 3–4 ml min⁻¹. Neurons in the SI or HDB were visually identified with a 60 \times water-immersion objective attached to an upright microscope (BX50WI, Olympus Optics, Tokyo, Japan). Images were detected with a cooled CCD camera (CCD-300T-RC, Nippon Roper, Tokyo, Japan) and displayed on a video monitor (LC-150M1, Sharp, Osaka, Japan). Cy3-192IgG-labeled neurons were visualized using the appropriate fluorescence filter. Patch pipettes were made from standard-walled borosilicate glass capillaries (1.5 mm OD; Clark Electromedical, Reading, UK). For the recording of evoked or miniature synaptic currents, patch pipettes were filled with an internal solution of the following composition (in mM): CsCl, 140; NaCl, 9; Cs-EGTA, 1; Cs-HEPES, 10; Mg-ATP, 2 (pH adjusted with 1 M CsOH). Whole cell recordings were made from neurons labeled with Cy3-192IgG (Fig. 1, A and B) using a patch-clamp amplifier (Axopatch 200B, Axon Instruments, Foster City, CA). For the recording of the membrane properties and action potentials of the labeled neurons, another internal solution of the following composition (in mM) was used: KMeSO₄, 135; KCl, 5; NaCl, 5; CaCl₂, 0.1; K-EGTA, 1; K-HEPES, 5; Mg-ATP, 5; and Na₃-GTP, 0.5 (pH adjusted with 1 M KOH). The cell capacitance and the series resistance were measured from the amplifier. The access resistance was monitored by measuring capacitive transients obtained in response to a hyperpolarizing voltage step (5 mV, 25 ms) from the holding potential of -65 mV. No correction was made for the liquid junction potentials (calculated to be 5.0 mV by pCLAMP7 software, Axon Instruments). Synaptic currents were evoked by delivering voltage pulses (0.2–0.4 ms in duration) of suprathreshold intensity at 0.2 Hz extracellularly by a stimulating electrode, made from the same glass capillary as for the recording pipette and filled with 1 M NaCl. The stimulating electrode was placed within a 50- to 120- μ m radius of the recorded neuron. The position of the stimulating electrode was varied until a stable response was evoked in the recorded neuron. All the inhibitory and excitatory postsynaptic currents (IPSCs and EPSCs, respectively) were evoked at a holding

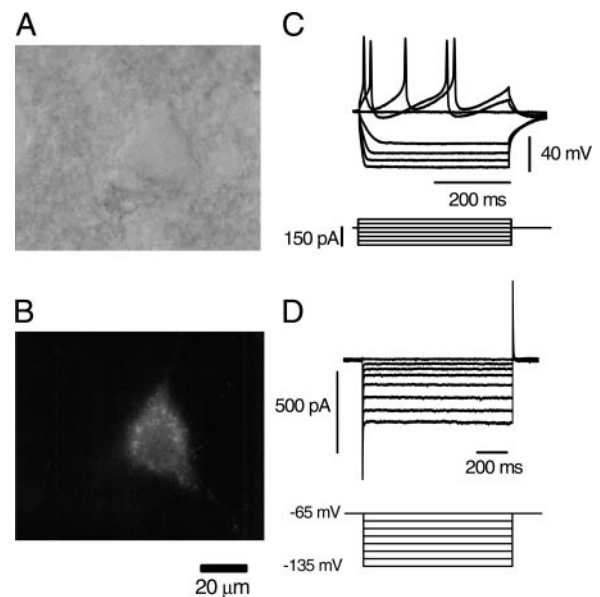


FIG. 1. Labeling of a cholinergic neuron in the basal forebrain (BF) using Cy3-192IgG, a selective marker of p75-receptor-expressing neuron, and electrophysiological properties of the labeled neuron. *A*: BF neuron viewed under IR-DIC microscopy. *B*: same neuron as in *A* in a fluorescent image labeled with Cy3-192IgG. *C*: membrane potentials and action potentials recorded in the current-clamp mode from another BF neuron labeled with Cy3-192IgG in response to the hyperpolarizing and depolarizing current pulses (bottom traces). Note the presence of inward rectification that is characteristic of cholinergic neurons in the BF. *D*: membrane currents recorded from another BF neuron labeled with Cy3-192IgG in the voltage-clamp mode. Neuron was held at -65 mV and hyperpolarizing voltage-step pulses (bottom traces) were applied through the recording pipette. Note the presence of inward rectification also in the voltage-clamp mode. Slice was 300 μ m in thickness and obtained from 20-day-old (*A–C*) and 18-day-old (*D*) rat brain. Cy3-192IgG (3 μ l) was injected into the lateral ventricle of the same side 4 days (*A–C*) and 5 days (*D*) before the slice preparation.

potential of -65 mV. Experiments were carried out at room temperature (21–26°C).

Data were stored on digital-audio tapes using a DAT recorder (DC to 10 kHz; Sony, Tokyo, Japan). Evoked IPSCs and EPSCs were digitized off-line at 10 kHz (low-pass filtered at 2 kHz with an eight-pole Bessel filter) using pCLAMP8 software (Axon Instruments). The effects of SS or SS-receptor (*sst*) agonists on the evoked IPSCs or EPSCs was assessed by averaging the amplitude of IPSCs or EPSCs for 100 s (20 traces) during the peak response to each agonist and comparing this value with the averaged amplitude of 20 traces just before the agonist application. Miniature IPSCs and EPSCs (mIPSCs and mEPSCs, respectively) were filtered at 2 kHz and digitized at 20 kHz using pCLAMP8 software. The analyses of mIPSCs and mEPSCs were carried out using N software provided by Dr. S. F. Traynelis (Emory University). The effect of SS on mIPSCs or mEPSCs was assessed by comparing the frequency and amplitude distribution of the events for 5–10 min during the peak responses to SS with those obtained just before drug application. Statistical analysis was carried out using both Student's *t*-test (two-tailed) and a nonparametric Mann-Whitney *U* test. The Kolmogorov-Smirnov (K-S) test was used for comparison of cumulative probability distribution of mIPSCs and mEPSCs. In all statistics, a *P* value of 0.05 was used as the confidence limit. Data are expressed as means \pm SE.

Drugs

Cy3-192IgG was custom synthesized by Advanced Targeting Systems (San Diego, CA). Other drugs were stored in frozen stock solution and dissolved in the perfusing solution just before application

in the final concentration indicated. All drugs were applied in the bath. Somatostatin was purchased from Peptide Institute (Osaka, Japan). 6-Cyano-7-nitroquinoxaline-2,3-dione (CNQX), D-(–)-2-amino-5-phosphonopentanoic acid (D-AP5), octreotide, seglitide, and CYN 164806 were from Tocris Cookson (Bristol, UK). Bicuculline methochloride and strychnine were from Sigma (St. Louis, MO). Tetrodotoxin (TTX) was from Sankyo (Tokyo, Japan).

RESULTS

Cell identification

Whole cell recordings were made from a total of 94 Cy3-192IgG-stained neurons within the HDB or SI of the BF region. Figure 1, *A* and *B* shows a BF neuron under IR-DIC and stained with Cy3-192IgG. Membrane properties and action potential firing were examined in the current-clamp mode or voltage-clamp mode with KMeSO₄-based internal solution in 28 of these 94 neurons. In current clamp, hyperpolarizing current injections produced inward rectification and depolarizing current injection evoked action potentials in all of the 18 neurons tested (Fig. 1*C*). The inwardly rectifying currents were also observed in the voltage-clamp mode in all of the 10 neurons tested (Fig. 1*D*). Electrophysiological properties of all these 28 neurons (Fig. 1, *C* and *D*) agreed with those previously reported on cholinergic neurons within the BF region (Bengtson and Osborne 2000; Wu et al. 2000). Therefore Cy3-192IgG-positive cells were identified as cholinergic neurons and used in the following experiments on SS-induced modulation of synaptic currents.

Effect of SS on the evoked IPSCs

After whole cell configuration was made from BF neurons stained with Cy3-192IgG, synaptic currents were evoked by focal stimulation in the presence of CNQX (5 μM), D-AP5 (25 μM), and strychnine (0.5 μM) to block non-NMDA (*N*-methyl-D-aspartate), NMDA, and glycinergic current components, respectively. The amplitude of the evoked synaptic currents was -369.9 ± 33.6 pA ($n = 26$). These synaptic currents were reversibly blocked by bath application of bicuculline (10 μM) in all of the four neurons tested (Fig. 2, *A1* and *A2*), confirming that they were GABA_A-receptor-mediated IPSCs. Bath application of somatostatin (SS, 1 μM) gradually reduced the amplitude of the evoked IPSCs, and the effect reached its steady state in several minutes (Fig. 2, *B1* and *B2*). The IPSCs recovered to the control level after 5- to 10-min washout of SS (Fig. 2, *B1* and *B2*). The magnitude of inhibition of the evoked IPSCs by SS (1 μM) was $34.4 \pm 2.14\%$ ($n = 16$, Fig. 7*Ab*). SS had no effect on the holding current with the present CsCl-based internal solution at the holding potential of -65 mV.

Effect of SS on the spontaneous mIPSCs

To dissect out whether the site of SS-induced action was pre- or postsynaptic, the effect of SS on the mIPSCs was examined in the presence of tetrodotoxin (TTX, 0.5 μM) in addition to CNQX (5 μM), D-AP5 (25 μM), and strychnine (0.5 μM). The frequency of mIPSCs was 0.65 ± 0.10 Hz ($n = 15$) in normal

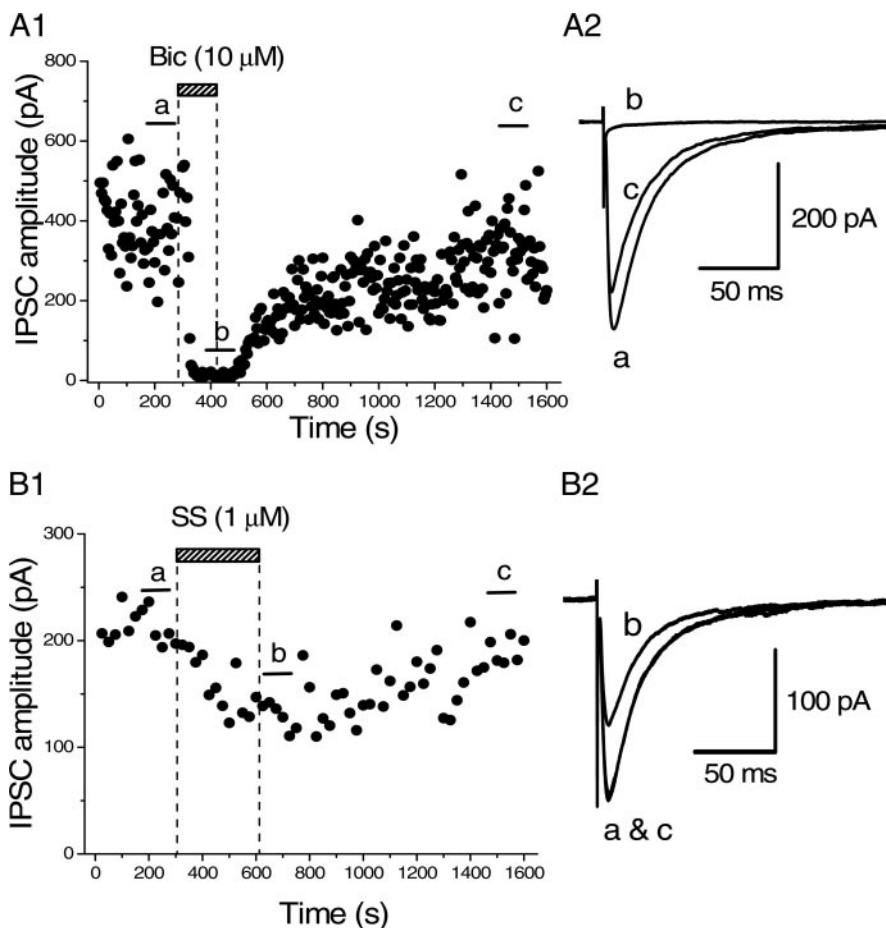


FIG. 2. Effect of somatostatin (SS) on GABAergic inhibitory postsynaptic currents (IPSCs) evoked in BF neurons stained with Cy3-192IgG. *A1*: time course of blockade of the evoked synaptic currents by bicuculline (10 μM, Bic). Synaptic currents were evoked by focal stimulation in the presence of 6-cyano-7-nitroquinoxaline-2,3-dione (CNQX, 5 μM), D-(–)-2-amino-5-phosphonopentanoic acid (D-AP5, 25 μM), and strychnine (0.5 μM) to block non-NMDA (*N*-methyl-D-aspartate) glutamatergic, NMDA glutamatergic, and glycinergic components, respectively. Holding potential was -65 mV. Each point in the time course shows the amplitude of the synaptic currents evoked at 0.2 Hz (every 5 s). Bic applied in the bath during the indicated period reversibly blocked the synaptic currents. *A2*: superimposed averaged traces of 20 consecutive responses evoked during the periods indicated in *A1* (*a–c*). Blockade by Bic suggests that these synaptic currents were γ -aminobutyric acid type A (GABA_A)-receptor-mediated inhibitory postsynaptic currents (IPSCs). *B1*: time course of inhibition of the IPSCs (evoked in another BF neuron stained with Cy3-192IgG) by SS. Each point in the time-course plot represents the mean amplitude of 5 consecutive IPSCs evoked at 0.2 Hz. Bath application of SS (1 μM) during the indicated period gradually suppressed the IPSCs and the effect reached a steady state in 5 min. IPSCs recovered from SS-induced inhibition after 10-min washout. *B2*: averages of 20 consecutive IPSCs during the indicated periods in *B1* (*a–c*). In this neuron, SS (1 μM) inhibited the IPSCs by 38.3%. Superimposed traces of *a* and *c* in *B2* show that the recovery was perfect. Pooled data from 16 cells yielded the inhibition of $34.4 \pm 2.14\%$ (means \pm SE) by 1 μM SS. No effect was observed on the holding current by SS application with CsCl-based internal solution at -65 mV.

Ca^{2+} (2.4 mM) external solution. Bath application of SS (1 μM) reduced the frequency of mIPSCs and the effect reached its steady state in 3–5 min (Fig. 3, *A* and *B*). The magnitude of inhibition of the mIPSC frequency by SS was $44.1 \pm 3.72\%$ ($n = 10$) in normal (2.4 mM) Ca^{2+} concentration. On the other hand, SS had no significant effect on the amplitude distribution or mean amplitude of mIPSCs (Fig. 3, *C* and *D*). The relative amplitude of mIPSCs during application of SS was $102.3 \pm 3.59\%$ ($n = 10$) of the control value in the 2.4 mM Ca^{2+} -containing solution.

Effect of SS on the evoked EPSCs

Synaptic currents were evoked in Cy3-192IgG-labeled BF neurons by focal electrical stimulation in the presence of bicuculline (10 μM), strychnine (0.5 μM), and D-AP5 (25 μM) to block GABA_A-, glycine-, and NMDA-receptor-mediated current components, respectively. The amplitude of the evoked synaptic currents was -104.5 ± 11.2 pA ($n = 16$). As shown in Fig. 4, *A1* and *A2*, these synaptic currents were reversibly blocked by bath application of CNQX (5 μM) in all of the four neurons tested, confirming that they were non-NMDA glutamatergic EPSCs. Similarly to the case of IPSCs, bath application of SS (1 μM) also inhibited the amplitude of evoked EPSCs in a reversible manner (Fig. 4, *B1* and *B2*). The magnitude of inhibition of the evoked EPSCs by SS (1 μM) was $34.1 \pm 2.62\%$ ($n = 15$, Fig. 7*Bb*).

Effect of SS on the spontaneous mEPSCs

The effect of SS on the mEPSCs was also examined in the presence of TTX (0.5 μM) in addition to bicuculline (10 μM), D-AP5 (25 μM), and strychnine (0.5 μM). The frequency of mEPSCs was 1.17 ± 0.23 Hz ($n = 11$) in normal Ca^{2+} (2.4 mM) external solution. Bath application of SS (1 μM) reduced the frequency of mEPSCs and the effect reached its steady state in 3–5 min (Fig. 5, *A* and *B*). The inhibition of the mEPSC frequency by SS was $50.1 \pm 2.95\%$ ($n = 11$) in normal (2.4 mM) Ca^{2+} concentration. Similarly to

the case of mIPSCs, SS had no significant effect on the amplitude distribution or mean amplitude of mIPSCs (Fig. 5, *C* and *D*). The relative amplitude of mIPSCs during application of SS was $97.8 \pm 2.72\%$ ($n = 11$) of the control value, in 2.4 mM Ca^{2+} -containing solution.

Ca^{2+} dependency of SS-induced effects on mIPSCs and mEPSCs

The present results concerning SS-induced effects on mIPSCs and mEPSCs suggest that SS's action is presynaptically mediated. To investigate whether the presynaptic action of SS is targeted at Ca^{2+} entry into the presynaptic terminal, we next examined the external Ca^{2+} concentration dependency of SS-induced effect on the mIPSCs and mEPSCs. After confirming SS-induced effect and recovery with washout in normal (2.4 mM) Ca^{2+} -containing solution, the external Ca^{2+} concentration was raised to 7.2 mM in the same neuron and SS was applied again. Furthermore, in this series of experiments, sucrose was added in the normal solution to make it isotonic with the high- Ca^{2+} solution. The frequency of mIPSCs increased from 0.68 ± 0.13 Hz ($n = 6$) to 1.61 ± 0.46 Hz ($n = 6$) when external Ca^{2+} concentration was raised to 7.2 mM. In the solution containing 7.2 mM Ca^{2+} , SS inhibited the frequency of mIPSCs by $74.6 \pm 3.32\%$ ($n = 6$) of control, significantly ($P < 0.05$) larger than that in normal Ca^{2+} concentration ($44.7 \pm 2.54\%$, $n = 6$, Fig. 6*A*). The relative amplitude of mIPSCs during application of SS was $100.8 \pm 4.04\%$ ($n = 6$), and $101.9 \pm 1.91\%$ ($n = 6$) of the respective control value, in 2.4 and 7.2 mM Ca^{2+} -containing solution, respectively.

Similarly to the case of mIPSCs, the frequency of mEPSCs increased from 0.99 ± 0.17 Hz ($n = 6$) in normal Ca^{2+} (2.4 mM) solution to 1.95 ± 0.73 Hz ($n = 6$) in the high- Ca^{2+} (7.2 mM) external solution. The inhibition of the mEPSC frequency by SS was $47.6 \pm 1.87\%$ ($n = 6$) and $69.7 \pm 2.81\%$ ($n = 6$) of control in 2.4 and 7.2 mM Ca^{2+} concentration, respectively (Fig. 6*B*). SS-induced inhibition of mEPSC frequency was significantly ($P < 0.05$) larger in 7.2 mM Ca^{2+} -containing solution than in normal Ca^{2+} concentration (Fig. 6*B*). The

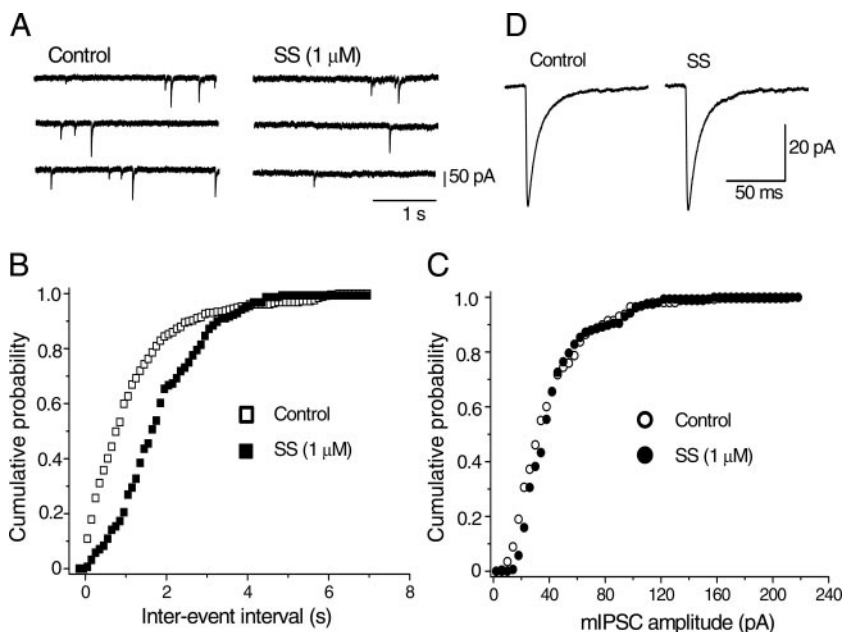


FIG. 3. Effect of SS on the miniature IPSCs (mIPSCs) recorded in a BF neuron stained with Cy3-192IgG. mIPSCs were recorded in 2.4 mM CaCl_2 -containing external solution in the presence of tetrodotoxin (TTX, 0.5 μM), CNQX (5 μM), D-AP5 (25 μM), and strychnine (0.5 μM). Holding potential was -65 mV. *A*: consecutive traces recorded before and 6 min after application of 1 μM SS. *B* and *C*: cumulative probability distribution of interevent intervals (*B*) and peak amplitudes (*C*) of mIPSCs from the same neuron shown in *A*, comparing distributions in the absence (open symbols) and presence (filled symbols) of SS. Control data contain 258 events per 5-min period; data in the presence of SS contain 157 events per 5-min period. Inter-event interval was increased (i.e., the frequency was decreased), whereas the distribution of mIPSC amplitude was unaffected by SS, suggesting that SS presynaptically inhibits GABA release. *D*: averaged mIPSCs in control (258 events) and during application of SS (157 events). Mean amplitude of mIPSCs was unaffected by SS.

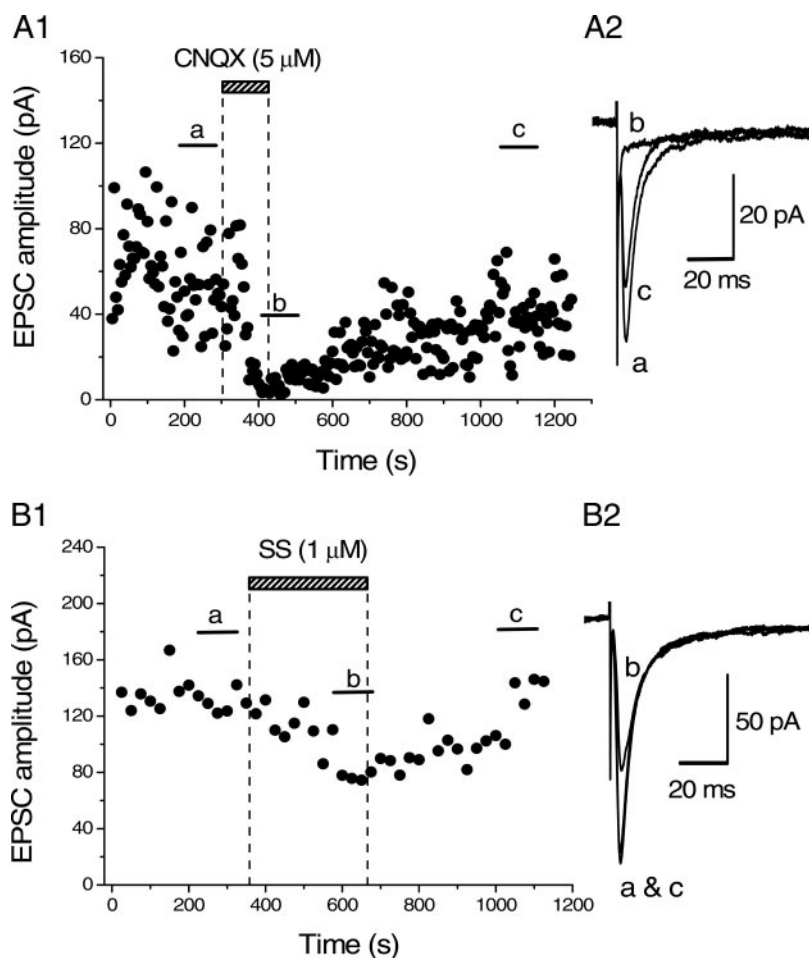


FIG. 4. Effect of SS on the evoked non-NMDA glutamatergic excitatory postsynaptic currents (EPSCs). *A1*: time course of blockade of the evoked synaptic currents by CNQX ($5 \mu\text{M}$). Synaptic currents were evoked by focal stimulation in the presence of D-AP5 ($25 \mu\text{M}$), bicuculline ($10 \mu\text{M}$), and strychnine ($0.5 \mu\text{M}$) to block NMDA glutamatergic, GABA_A-receptor-mediated, and glycinergic components, respectively. Holding potential was -65 mV . Each point in the time course shows the amplitude of the synaptic currents evoked at 0.2 Hz (every 5 s). CNQX applied in the bath during the indicated period reversibly blocked the synaptic currents, suggesting that these synaptic currents were non-NMDA glutamate receptor-mediated EPSCs. *A2*: superimposed averaged traces of 20 consecutive responses evoked during the periods indicated in *A1* (*a-c*). *B1*: time course of inhibition of the EPSCs (evoked in another BF neuron stained with Cy3-192IgG) by SS. Each point in the time-course plot represents the mean amplitude of 5 consecutive EPSCs evoked at 0.2 Hz . Bath application of SS ($1 \mu\text{M}$) during the indicated period gradually suppressed the EPSCs and the effect reached a steady state in 5 min. EPSCs recovered from SS-induced inhibition after 7-min washout. *B2*: averages of 20 consecutive EPSCs during the indicated periods in *B1* (*a-c*). In this neuron, SS ($1 \mu\text{M}$) inhibited the EPSCs by 35.9%. Superimposed traces of *a* and *c* in *B2* show that the recovery was perfect. Pooled data from 15 cells yielded the inhibition of $34.1 \pm 2.62\%$ (means \pm SE) by $1 \mu\text{M}$ SS.

relative amplitude of mEPSCs during application of SS was $99.1 \pm 4.68\%$ ($n = 6$), and $101.7 \pm 2.33\%$ ($n = 6$) of the respective control value, in 2.4 and 7.2 mM Ca^{2+} -containing solution, respectively.

Pharmacological identification of SS-receptor subtypes

Although there is a lack of highly selective SS-receptor-related drugs, some drugs are available for elucidating SS-

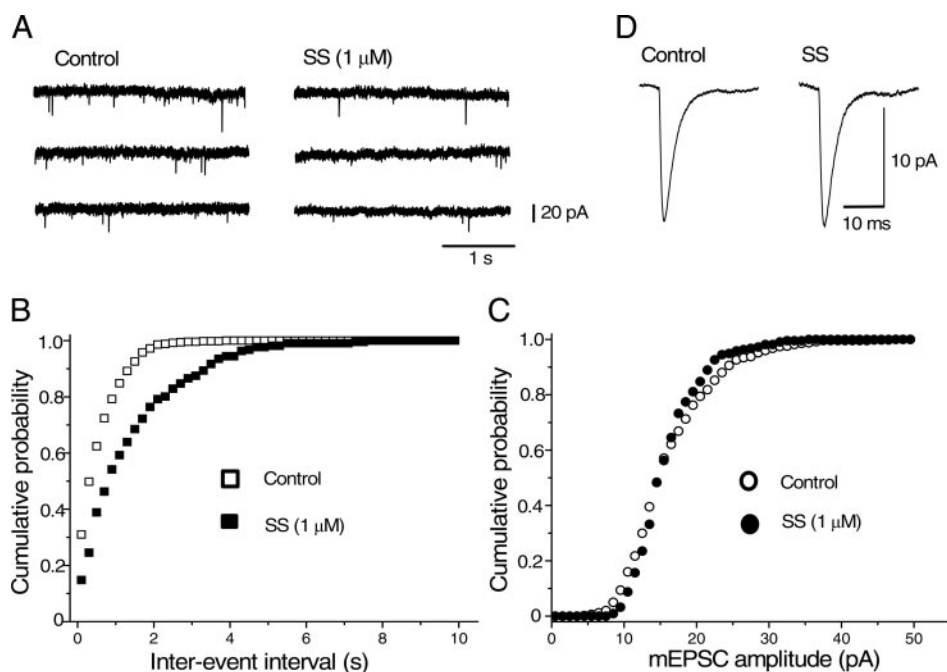


FIG. 5. Effect of SS on the spontaneous miniature non-NMDA glutamatergic EPSCs (mEPSCs). mEPSCs were recorded in 2.4 mM CaCl_2 -containing external solution in the presence of TTX ($0.5 \mu\text{M}$), bicuculline ($10 \mu\text{M}$), D-AP5 ($25 \mu\text{M}$), and strychnine ($0.5 \mu\text{M}$). Holding potential was -65 mV . *A*: consecutive traces recorded before and 5 min after application of $1 \mu\text{M}$ SS. *B* and *C*: cumulative probability distribution of interevent intervals (*B*) and peak amplitudes (*C*) of mEPSCs from the same neuron shown in *A*, comparing distributions in the absence (open symbols) and presence (filled symbols) of SS. Control data contain 501 events per 5-min period; data in the presence of SS contain 217 events per 5-min period. Interevent interval was increased (i.e., the frequency was decreased), whereas the distribution of mEPSC amplitude was unaffected by SS, suggesting that SS presynaptically inhibits glutamate release. *D*: averaged mEPSCs in control (501 events) and during application of SS (217 events). Mean amplitude of mEPSCs was unaffected by SS.

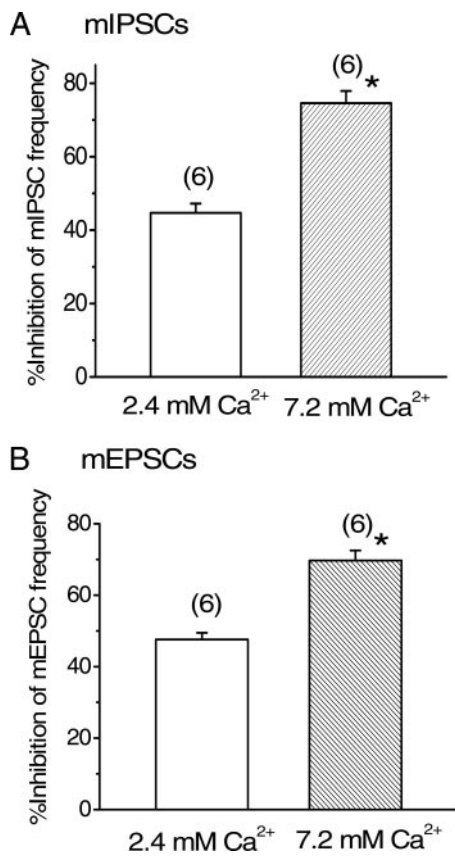


FIG. 6. Ca^{2+} dependency of SS-induced effect on the frequency of mIPSCs and mEPSCs. Histograms summarizing the inhibitory effect of SS on the frequency of mIPSCs (A) and mEPSCs (B) in 2.4 and 7.2 mM Ca^{2+} . A: values for 2.4 and 7.2 mM Ca^{2+} were $44.7 \pm 2.54\%$ ($n = 6$) and $74.6 \pm 3.32\%$ ($n = 6$), respectively. Effect in 7.2 mM Ca^{2+} (*) was significantly ($P < 0.05$) larger than that in 2.4 mM Ca^{2+} . B: effect in 7.2 mM Ca^{2+} ($69.7 \pm 2.81\%$, $n = 6$, *) was significantly ($P < 0.05$) larger than that in 2.4 mM Ca^{2+} ($47.6 \pm 1.87\%$, $n = 6$).

receptor subtypes (*sst*) mediating SS-induced inhibition of IPSCs or EPSCs. Therefore we examined the effects of two agonists, octreotide and seglitide, on the IPSCs and EPSCs, and one antagonist, CYN 154806, on the SS-induced inhibition

of IPSCs and EPSCs. Octreotide is not expected to mimic the actions of SS if they are mediated by *sst*₁ or *sst*₄ subtypes, whereas seglitide will not mimic *sst*₁-mediated actions (Hannon et al. 2002; Raynor et al. 1993). CYN154806 should block only *sst*₂ subtype (Hannon et al. 2002; Mastrodimou et al. 2006; Nunn et al. 2002).

IPSCs. First, the effects of octreotide and seglitide on the amplitude of IPSCs were compared with those on SS (Fig. 7A). Octreotide at a concentration of 1 μM inhibited IPSCs by $29.2 \pm 5.11\%$ ($n = 6$, Fig. 7A). Seglitide (1 μM) also inhibited the IPSCs by $30.2 \pm 10.1\%$ ($n = 5$, Fig. 7A). The effect of octreotide or seglitide was not significantly ($P > 0.05$) different from that of SS ($34.4 \pm 2.14\%$, $n = 16$, Fig. 7A). These results suggest that SS-induced action on the IPSCs is not mediated by *sst*₁ or *sst*₄ subtypes. To further examine this possibility, the effect of CYN 154806 (1 μM) on SS (1 μM)-induced inhibition of IPSCs was examined (Fig. 8A). After confirming the effect of SS and recovery on washout, the antagonist was applied for 10 min, and then SS was applied again in the presence of the antagonist. Application of CYN 154806 itself had no effect on the IPSCs in any of six neurons tested. In the presence of CYN 154806, SS-induced inhibitory effect on the IPSCs was reduced to $11.2 \pm 1.21\%$ ($n = 6$, Fig. 8A), which was significantly ($P < 0.05$) smaller than that of SS alone obtained in the corresponding six neurons ($39.4 \pm 3.64\%$, Fig. 8A). These results suggest that SS-induced action of the IPSCs is mediated mostly by the *sst*₂ subtype.

EPSCs. Similarly to IPSCs, the effects of octreotide and seglitide on the amplitude of EPSCs were examined. Unlike the case of IPSCs, octreotide- or seglitide-induced inhibitory effect was not prominent. The inhibition of EPSCs by octreotide (1 μM) or seglitide (1 μM) was $8.12 \pm 5.11\%$ ($n = 6$) or $8.83 \pm 2.92\%$ ($n = 6$), respectively, which was significantly ($P < 0.05$) smaller than that by SS (1 μM , $34.1 \pm 2.62\%$, $n = 15$, Fig. 7B). Furthermore, even in the presence of CYN 154806 (1 μM), SS still inhibited the EPSCs by $32.9 \pm 4.66\%$ ($n = 6$, Fig. 8B), which was not significantly ($P > 0.05$) different from the value with SS alone in the corresponding six neurons

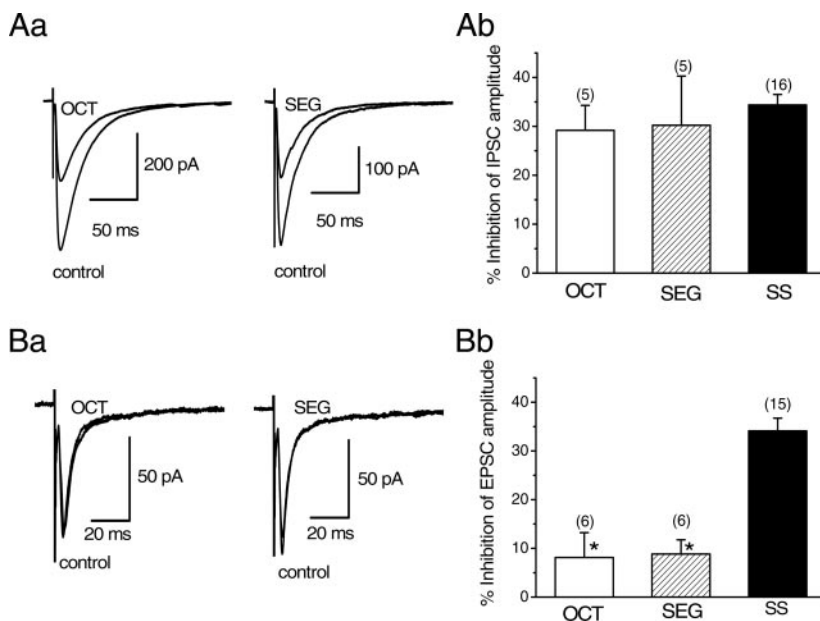


FIG. 7. Effects of octreotide (OCT) and seglitide (SEG) on the IPSCs and EPSCs. All IPSCs or EPSCs were evoked at 0.2 Hz at the holding potential of -65 mV. A: inhibitory effects of OCT and SEG on the IPSCs. B: lack of effect of OCT or SEG on the EPSCs. Each trace in Aa and Ba is the superimposed averages of 20 consecutive synaptic currents before (control) and during agonist application (OCT or SEG). Ab and Bb: histograms summarizing the mean inhibitory effects of OCT, SEG, and somatostatin (SS) on the IPSCs (Ab) and EPSCs (Bb). Error bars indicate SE. Concentration of each agonist was 1 μM . Ab: values for OCT and SEG were $29.2 \pm 5.11\%$ ($n = 5$) and $30.2 \pm 10.1\%$ ($n = 5$), respectively, which were not significantly ($P > 0.05$) different from that of SS ($34.4 \pm 2.14\%$, $n = 16$). Bb: values for OCT and SEG were $8.12 \pm 5.11\%$ ($n = 6$) and $8.83 \pm 2.92\%$ ($n = 6$), respectively, which were significantly ($*P < 0.05$) smaller than that of SS ($34.1 \pm 2.62\%$, $n = 15$).

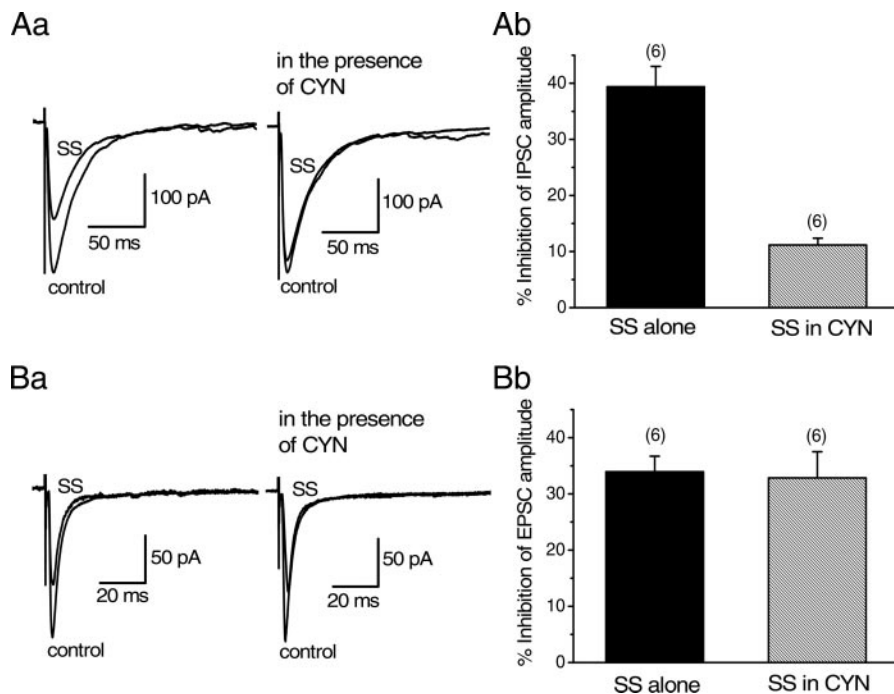


FIG. 8. Effect of CYN154806 (CYN) on SS-induced inhibition of IPSCs and EPSCs. Effect of SS (1 μ M) on IPSCs (A) or EPSCs (B) in the presence of CYN (1 μ M) was compared with that of SS alone. All IPSCs or EPSCs were evoked at 0.2 Hz. Holding potential was -65 mV. Each trace in Aa and Ba is the superimposed averages of 20 consecutive synaptic currents before (control) and during SS application. CYN was applied for 10 min before second application of SS. Ab and Bb: histograms summarizing the mean inhibitory effects of SS on IPSCs (Ab) and EPSCs (Bb) in the absence and presence of CYN. Error bars indicate SE. Ab: value in the presence of CYN was $11.2 \pm 1.21\%$ ($n = 6$), which was significantly ($*P < 0.05$) smaller than that of SS alone in the corresponding neurons ($39.4 \pm 3.64\%$, $n = 6$). Bb: value in the presence of CYN ($32.9 \pm 4.66\%$, $n = 6$) was not significantly ($P > 0.05$) different from that of SS alone in the corresponding neurons ($34.0 \pm 2.76\%$, $n = 6$).

($34.0 \pm 2.76\%$, $n = 6$, Fig. 8B). These results suggest that *sst* receptor subtypes mediating SS-induced inhibition of EPSCs are mainly *sst*₁ or *sst*₄.

DISCUSSION

The present findings demonstrate that exogenously applied SS presynaptically inhibits both GABA and glutamate release onto BF cholinergic neurons. They also suggest that SS-induced inhibition of GABA and glutamate release is mediated by different subtypes of *sst* receptors. The present results on the mIPSCs and mEPSCs suggest that SS action on the transmission is mediated in a calcium-dependent way. It remains to be elucidated whether activation of presynaptic *sst* receptors actually leads to blockade certain types of calcium channels. Although presynaptic modulation by SS has been reported in several central excitatory or inhibitory synapses, including hippocampus (Boehm and Betz 1997; Tallent and Siggins 1997), sensory thalamus (Leresche et al. 2000), hypothalamus (Lanneau et al. 2000), and the reticular thalamic nucleus (Sun et al. 2002), a potential role for SS in the modulation of BF synaptic transmission has been demonstrated for the first time in the present study. Indeed, the modulatory role of SS for inhibiting both GABA and glutamate release onto the BF cholinergic neurons should be unique.

GABAergic and glutamatergic afferents to BF cholinergic neurons

Cholinergic neurons in the ventral pallidum and substantia innominata receive heavy GABA input (Zaborszky et al. 1986) that originates in part from GABAergic neurons of the nucleus accumbens (Zaborszky and Cullinan 1992). An additional source of GABA input to cholinergic neurons may be local collaterals of parvalbumin-containing projection neurons. Indeed, it has been shown that juxtacellularly filled parvalbumin

neurons give off axon collaterals in BF areas (Zaborszky and Duque 2000).

A potential direct source of glutamatergic input to BF cholinergic neurons may be amygdalofugal axons because such axons have been found to form asymmetric synapses on cholinergic neurons in the ventral pallidum (Zaborszky et al. 1984); and amygdaloid lesions have been found to result in decreased glutamate uptake in the substantia innominata (Francis et al. 1987). In addition, it has been suggested that putative glutamatergic afferents from the mesopontine tegmentum could affect cortical ACh release by basal forebrain cholinergic neurons (Rasmusson et al. 1994), although no direct morphological evidence supports this notion. Furthermore, glutamatergic afferents to BF cholinergic neurons may originate from local Vglut2 neurons (Hur and Zaborszky 2005).

Mechanism of SS action on GABA and glutamate release

The present electrophysiological results show that exogenously applied SS presynaptically inhibits both GABA and glutamate release onto cholinergic neurons in the BF. Electrophysiological properties of the BF neurons identified by Cy3-192IgG well agreed with those reported previously (Bengtson and Osborne 2000), confirming that Cy3-192IgG is a good marker for the identification of cholinergic neurons in the BF (Wu et al. 2000).

The functional effects of SS are exerted by G-protein-coupled receptors. There are five cloned subtypes of *sst* receptors (*sst*₁₋₅) in the CNS (Dournaud et al. 2000). In previous studies using subtype-specific antibodies, abundant *sst*₁ and *sst*_{2A} immunoreactivity was seen in nerve processes in the substantia innominata and in the area ventral to HDB (Dournaud et al. 2000; Hervieu and Emson 1998), suggesting that the presynaptic action of SS on GABA and glutamate release may be mediated through presynaptic *sst*₁₋₂ receptors located on GABAergic or glutamatergic axons impinging on cholinergic

neurons in these BF regions. The present pharmacological analyses using *sst*-receptor-specific drugs could provide more detailed insights that SS-induced inhibition of GABA and glutamate release is mediated by different *sst* subtypes; SS-induced inhibition of GABA release is mediated by mostly *sst*₂ receptors, whereas the inhibition of glutamate release is mainly mediated by *sst*₁ or *sst*₄ receptors. The present finding of *sst*₂-receptor-mediated inhibition of GABA release well agrees with a recent study by Bassant et al. (2005). The work has demonstrated that GABAergic neurons in the medial septum/diagonal band of Broca express *sst*_{2A} receptors, activation of which by octreotide inhibits the activities of the GABAergic neurons. The present data suggest that SS has a role in modulating the excitability of BF cholinergic neurons by inhibiting both inhibitory and excitatory transmissions, as reported in the case of dopamine (Momiya and Sim 1996; Momiya et al. 1996). Thus it is likely that SS acts to balance between excitatory and inhibitory inputs to BF cholinergic neurons. Although no postsynaptic effects were observed in the present electrophysiological studies using CsCl-based internal solution, we have observed in our preliminary experiments using K-based internal solution that SS (1 μ M) hyperpolarized the membrane of putative cholinergic neurons in the BF in a similar time course to that required to reduce transmitter release (unpublished observations). Detailed mechanisms underlying postsynaptic effects of SS remain to be elucidated to construct a complete picture of SS's role in controlling the excitability of BF cholinergic neurons.

At present the mechanism of how endogenous SS release can influence GABA or glutamate release onto cholinergic neurons is unclear. Actually, the present study does not show that synaptically released SS can affect transmission. Thus it seems unlikely that synaptically released SS would inhibit excitatory and inhibitory transmission onto the same neuron to the same extent. With respect to the functional interpretation of SS action on cholinergic neurons, it is important to know whether the SS terminals on cholinergic neurons coexpress GABA. The most detailed study of GABA and SS coexistence to date has been done in the hippocampus (Esclapez and Houser 1995; Kosaka et al. 1988). According to these studies, 30–50% of dentate hilar GABA neurons contain SS, whereas the rest of GABA neurons contain other peptides.

Behavioral significance of SS/cholinergic interaction in the basal forebrain

Several behavioral studies suggest the role of SS in cognitive processes (DeNoble et al. 1989; Haroutunian et al. 1987; Malthe-Sorensen et al. 1978; Sunderland et al. 1987; Vecsei et al. 1984) or control of sleep conditions (Beranek et al. 1997; Hajdu et al. 2002). In addition the recent study mentioned above (Bassant et al. 2005) showed that intraseptal injections of octreotide or SS in freely moving rats reduce the power of hippocampal EEG in the theta band by activating *sst*_{2A} receptors, suggesting a mechanism in the control of theta activity. It might be possible that the effect of SS on sleep conditions is mediated at least partly by modulating the GABAergic/cholinergic interaction in the BF (Zaborszky et al. 1986).

For a comprehensive understanding of the behavioral relevance of GABA–SS–AOh–glutamate interactions in the BF, combined morphological–electrophysiological in vitro and in

vivo studies are necessary, which 1) identify the origin of SS input to BF cholinergic neurons, 2) determine the cellular and subcellular localization of SS receptors, 3) correlate the firing properties of SS and cholinergic neurons as they relate to EEG epochs along the entire sleep–wake cycle, and 4) establish the precise local synaptic circuitry of the BF.

ACKNOWLEDGMENTS

We are grateful to F. Nagy for constructive comments on the manuscript.

GRANTS

This work was supported by Grants-in-Aid (13680904 and 15016106) for Scientific Research from the Ministry of Education, Culture, Sports, Science, and Technology of Japan, Core Research for Evolutional Science and Technology of Japan Science and Technology Corporation, Astra Zeneca Research Grants 2001 and 2003 to T. Momiyama, and U.S. Public Health Service Grant NS-23945 to L. Zaborszky.

REFERENCES

- Bassant M-H, Simon A, Poindessous-Jazat F, Csaba Z, Epelbaum J, and Dournaud P. Medial septal GABAergic neurons express the somatostatin *sst*_{2A} receptor: functional consequences on unit firing and hippocampal theta. *J Neurosci* 25: 2032–2041, 2005.
- Bengtson CP and Osborne PB. Electrophysiological properties of cholinergic and noncholinergic neurons in the ventral pallidum region of the nucleus basalis in rat brain slice. *J Neurophysiol* 83: 2649–2660, 2000.
- Beranek L, Obal F Jr, Taishi P, Bodosi B, Laczi F, and Krueger JM. Changes in rat sleep after single and repeated injections of the long-acting somatostatin analog octreotide. *Am J Physiol* 273: 1484–1491, 1997.
- Boehm S and Betz H. Somatostatin inhibits excitatory transmission at rat hippocampal synapses via presynaptic receptors. *J Neurosci* 17: 4066–4075, 1997.
- Candy JM, Perry RH, Perry EK, Irving D, Blessed G, Fairbairn AF, and Tomlinson BE. Pathological changes in the nucleus of Meynert in Alzheimer's and Parkinson's disease. *J Neurol Sci* 59: 277–289, 1983.
- Chesselet MF and Graybiel AM. Striatal neurons expressing somatostatin-like immunoreactivity evidence for a peptidergic interneuronal system in the cat. *Neuroscience* 17: 547–571, 1986.
- Davies P and Terry RD. Cortical somatostatin-like immunoreactivity in cases of Alzheimer's disease and senile dementia of the Alzheimer type. *Neurobiol Aging* 2: 9–14, 1981.
- DeNoble VJ, Hepler DJ, and Barto RA. Cysteamine-induced depletion of somatostatin produces differential cognitive deficits in rats. *Brain Res* 482: 42–48, 1989.
- Dournaud P, Slama A, Beaudet A, and Epelbaum J. Somatostatin receptors. In: *Peptide Receptors. Part I. Handbook of Chemical Neuroanatomy*. Amsterdam: Elsevier, 2000, vol. 16, p. 1–43.
- Duque A, Balatoni B, Detari L, and Zaborszky L. EEG correlation of the discharge properties of identified neurons in the basal forebrain. *J Neurophysiol* 84: 1627–1635, 2000.
- Esclapez M and Houser CR. Somatostatin neurons are a subpopulation of GABA neurons in the rat dentate gyrus: evidence from colocalization of preprosomatostatin and glutamate decarboxylase messenger RNAs. *Neuroscience* 64: 339–355, 1995.
- Forloni G, Hohmann C, and Coyle JT. Developmental expression of somatostatin in mouse brain. I. Immunocytochemical studies. *Brain Res Dev Brain Res* 53: 6–25, 1990.
- Francis PT, Carl R, Pearson A, Lowe SL, Neal JW, Stephens PH, Powell TPS, and Bowen DM. The dementia of Alzheimer's disease: an update. *J Neurol Neurosurg Psychiatry* 50: 242–243, 1987.
- Hajdu I, Obal F Jr, Fang J, Krueger JM, and Rollo CD. Sleep of transgenic mice producing excess rat growth hormone. *Am J Physiol Regul Integr Comp Physiol* 282: R70–R76, 2002.
- Hannon JP, Nunn C, Stolz B, Bruns C, Weckbecker G, Lewis I, Troxler T, Hurth K, and Hoyer D. Drug design at peptide receptors: somatostatin receptor ligands. *Mol Neurosci* 18: 15–27, 2002.
- Haroutunian V, Kanof PD, and Davis KL. Interactions of forebrain cholinergic and somatostatinergic systems in the rat. *Brain Res* 496: 98–104, 1989.
- Haroutunian V, Mantin R, Campbell GA, Tsuboyama GK, and Davis KL. Cysteamine-induced depletion of central somatostatin-like immunoreactiv-

- ity: effects on behavior, learning, memory and brain neurochemistry. *Brain Res* 403: 234–242, 1987.
- Hendry SH, Jones EG, DeFelipe J, Schmechel D, Brandon C, and Emson PC.** Neuropeptide-containing neurons of the cerebral cortex are also GABAergic. *Proc Natl Acad Sci USA* 81: 6526–6530, 1984.
- Hervieu G and Emson PC.** The localization of somatostatin receptor 1 (sst₁) immunoreactivity in the rat brain using an N-terminal specific antibody. *Neuroscience* 85: 1263–1284, 1998.
- Hur E and Zaborszky L.** Vglut2 afferents to the medial prefrontal and primary somatosensory cortices: a combined retrograde tracing in situ hybridization study. *J Comp Neurol* 483: 351–373, 2005.
- Kapas L, Obal F Jr, Book AA, Schweitzer JB, Wiley RG, and Krueger JM.** The effects of immunolesions of nerve growth factor-receptive neurons by 192IgG-saporin in sleep. *Brain Res* 712: 53–59, 1996.
- Kohler C and Eriksson LG.** An immunohistochemical study of somatostatin and neurotensin positive neurons in the septal nuclei of the rat. *Anat Embryol (Berl)* 170: 1–10, 1984.
- Kosaka T, Wu JY, and Benoit R.** GABAergic neurons containing somatostatin-like immunoreactivity in the rat hippocampus and dentate gyrus. *Exp Brain Res* 71: 388–398, 1988.
- Kowall NW and Beal MF.** Cortical somatostatin, Neuropeptide Y, and NADPH diaphorase neurons: normal anatomy and alterations in Alzheimer's disease. *Ann Neurol* 23: 105–114, 1988.
- Lanneau C, Peineau S, Petit F, and Epelbaum J.** Somatostatin modulation of excitatory synaptic transmission between periventricular and arcuate hypothalamic nuclei in vitro. *J Neurophysiol* 84: 1464–1474, 2000.
- Leresche N, Asprodini E, Emri Z, Cope DW, and Crunelli V.** Somatostatin inhibits GABAergic transmission in the sensory thalamus via presynaptic receptors. *Neuroscience* 98: 513–522, 2000.
- Malthe-Sorensen D, Wood PL, Cheney DL, and Costa E.** Modulation of the turnover of acetylcholine in rat brain by intraventricular injections of thyrotropin-releasing hormone, somatostatin, neurotensin and angiotensin II. *J Neurochem* 31: 685–691, 1978.
- Manns ID, Alonso A, and Jones BE.** Discharge profiles of juxtacellularly labeled and immunohistochemically identified GABAergic basal forebrain neurons recorded in association with the electroencephalogram in anesthetized rats. *J Neurosci* 20: 9252–9263, 2000.
- Mastrodimou N, Kiagiadaki F, Hodjarova M, Karagianni E, and Thermos K.** Somatostatin receptors (sst₂) regulate cGMP production in rat retina. *Regul Pept* 133: 41–46, 2006.
- Momiyama T and Sim JA.** Modulation of inhibitory transmission by dopamine in rat basal forebrain nuclei: activation of presynaptic D₁-like dopaminergic receptors. *J Neurosci* 16: 7505–7512, 1996.
- Momiyama T, Sim JA, and Brown DA.** Dopamine D₁-like receptor-mediated presynaptic inhibition of excitatory transmission onto rat magnocellular basal forebrain neurones. *J Physiol* 495: 97–106, 1996.
- Momiyama T and Zaborszky L.** Somatostatin-induced presynaptic inhibition of excitatory and inhibitory transmission onto cholinergic neurons in the rat basal forebrain. *Neurosci Res Suppl* 26: S101, 2002.
- Momiyama T and Zaborszky L.** Somatostatin-induced presynaptic inhibition of GABA release onto cholinergic neurons in the rat basal forebrain. *Abstr 4th Forum Eur Neurosci* A048-24, 2004.
- Nunn C, Schoeffter P, Langenegger D, and Hoyer D.** Functional characterization of the peptide somatostatin sst₂ receptor antagonist CYN 154806. *Naunyn Schmiedeberg's Arch Pharmacol* 367: 1–9, 2002.
- Obal F Jr and Krueger JM.** Biochemical regulation of non-rapid-eye-movement sleep. *Front Biosci* 8: 520–550, 2003.
- Price DL, Whitehouse PJ, and Struble RG.** Cellular pathology in Alzheimer's and Parkinson's disease. *Trends Neurosci* 9: 29–33, 1986.
- Rasmusson DD, Clow K, and Szerb JC.** Modification of neocortical acetylcholine release and electroencephalogram desynchronization due to brain-stem stimulation by drugs applied to the basal forebrain. *Neuroscience* 60: 665–677, 1994.
- Raynor K, Murphy WA, Coy DH, Tayler JE, Moreau JP, Yasuda K, Bell GI, and Reisine T.** Cloned somatostatin receptors: identification of subtype-selective peptides and demonstration of high affinity binding of linear peptides. *Mol Pharmacol* 43: 838–844, 1993.
- Roberts GW, Crow TJ, and Polak JM.** Location of neuronal tangles in somatostatin neurones in Alzheimer's disease. *Nature* 314: 92–94, 1985.
- Rossor MN, Emson PC, Mountjoy CQ, Roth M, and Iversen LL.** Reduced amounts of immunoreactive somatostatin in the temporal cortex in senile dementia of Alzheimer type. *Neurosci Lett* 20: 373–377, 1980.
- Somogyi P, Hodgson AJ, Smith AD, Nunzi MG, Gorio A, and Wu JY.** Different populations of GABAergic neurons in the visual cortex and hippocampus of cat contain somatostatin- or cholecystokinin-immunoreactive material. *J Neurosci* 4: 2590–2603, 1984.
- Sun Q-Q, Huguenard JR, and Prince DA.** Somatostatin inhibits thalamic network oscillations *in vitro*: actions on the GABAergic neurons of reticular nucleus. *J Neurosci* 22: 5374–5386, 2002.
- Sunderland T, Rubinow DR, Tariot PN, Cohen RM, Newhouse PA, Mellow AM, Mueller EA, and Murphy DL.** CSF somatostatin in patients with Alzheimer's disease, older depressed patients, and age-matched control subjects. *Am J Psychiatry* 144: 1313–1316, 1987.
- Tallent MK and Siggins GR.** Somatostatin depresses excitatory but not inhibitory neurotransmission in rat CA1 hippocampus. *J Neurophysiol* 78: 3008–3018, 1997.
- Vecsei L, Bollok I, Varga J, Penke B, and Telegdy G.** The effect of somatostatin, its fragments and an analog on electroconvulsive shock-induced amnesia in rats. *Neuropeptides* 4: 137–143, 1984.
- Vincent SR, McIntosh CH, Buchan AM, and Brown JC.** Central somatostatin systems revealed with monoclonal antibodies. *J Comp Neurol* 238: 169–186, 1985.
- Wu M, Shanabrough M, Leranth C, and Alreja M.** Cholinergic excitation of septohippocampal GABA but not cholinergic neurons: implication for learning and memory. *J Neurosci* 20: 3900–3908, 2000.
- Zaborszky L and Cullinan WE.** Projections from the nucleus accumbens to cholinergic neurons of the ventral pallidum: a correlated light and electron microscopic double-immunolabelling study in rat. *Brain Res* 570: 92–101, 1992.
- Zaborszky L and Duque A.** Local synaptic connections of basal forebrain neurons. *Behav Brain Res* 115: 143–158, 2000.
- Zaborszky L and Duque A.** Sleep-wake mechanisms and basal forebrain circuitry. *Front Biosci* 8: 1146–1169, 2003.
- Zaborszky L, Heimer L, Eckenstein F, and Leranth C.** GABAergic input to cholinergic forebrain neurons: an ultrastructural study using retrograde tracing of HRP and double immunolabelling. *J Comp Neurol* 250: 282–295, 1986.
- Zaborszky L, Hur EE, Edwards RH, and Rommer E.** Glutamatergic innervation of basal forebrain cholinergic neurons. *Soc Neurosci Abstr* 29: 155.5, 2003.
- Zaborszky L, Leranth C, and Heimer L.** Ultrastructural evidence of amygdalofugal axonsterminating on cholinergic cells of the rostral forebrain. *Neurosci Lett* 52: 219–225, 1984.